# FUSE Fine Error Sensor Optical Performance

Jeffrey W. Kruk[a], Pierre Chayer[a], John Hutchings[b], Christopher Morbey[b], and Richard Murowinski[b]

[a]Center for Astrophysical Sciences, Department of Physics and Astronomy, The Johns Hopkins University, Baltimore, MD, USA

[b]National Research Council of Canada, Dominion Astrophysical Observatory, Herzberg Institute of Astrophysics, Victoria, BC, Canada

## ABSTRACT

The *Far Ultraviolet Spectroscopic Explorer* mission imposes stringent requirements on the satellite attitude control system. Target acquisition accuracy and target tracking stability must each be no greater than 0.5 arcseconds FWHM. The data required by the attitude control system to meet these requirements are provided by two redundant Fine Error Sensors. Each Fine Error Sensor operates as a slit-jaw camera that provides either complete images of the star-field around the line of sight of the telescope, or centroided positions of selected guide stars in the field of view.

The satellite pointing requirements must be met over a wide dynamic range of target or guide star brightness, for both sparse and crowded starfields, and for targets that may be either point sources or extended objects. We will describe the operational characteristics of the FES and present data on its performance. We also discuss the optical, mechanical, thermal, and electronic design challenges encountered in meeting the mission requirements, and how they were addressed in the context of a very tight development schedule.

**Keywords:** FUSE, Star Trackers, Optical Systems, Satellites

## 1. INTRODUCTION

The *Far Ultraviolet Spectroscopic Explorer* (FUSE) satellite is designed to obtain high-resolution far-ultraviolet (FUV) spectra of faint astronomical sources. To fulfill its science objectives, the FUSE satellite must be able to point its four co-aligned telescopes towards astronomical objects with an accuracy and stability of $0.5''$. The FUSE Fine Error Sensor (FES) is a visible light imaging camera that provides the data used by the attitude control system (ACS) to achieve this pointing accuracy. There are two redundant fine error sensors on FUSE: an active unit and a spare. The FES systems were provided to the FUSE project by the Canadian Space Agency (CSA), and were built by COM DEV Ltd. of Cambridge, Ontario. The FES conceptual design and detailed optical design were developed by the Dominion Astrophysical Observatory (DAO) of Victoria, British Columbia. The FUSE project was managed by the Johns Hopkins University (JHU).

Development work on the flight FES systems began in June 1996, with planned delivery dates of September and October 1997 for the two flight units. This aggressive schedule affected numerous design and implementation decisions, and necessitated close coordination among JHU, DAO, CSA, and COM DEV. Procurement delays of essential components delayed delivery of the flight systems until Spring 1998. These delays were accomodated by the satellite integration schedule by using the FES engineering qualification model for early system-level testing.

The rapid development schedule meant that interfaces between satellite subsystems had to be kept as simple as possible, and that the partitioning of functional responsibilities among subsystems had to permit development, integration, and testing of the different subsystems to proceed independently. The responsibility allocated to the FES is to provide two basic types of data: full field of view (FOV) images of the focal plane, and centroided positions of selected guide stars. All processing of these data to determine spacecraft attitude is performed by the Instrument Data System (IDS), a dedicated processor that controls all aspects of FUSE science data acquisition by means of a high-level scripting language and a suite of specialized data acquisition and data processing routines. The IDS is described by Heggestad and Moore (1999).[1]

Correspondence: E-mail: kruk@pha.jhu.edu

The partitioning of functions among the various subsystems helps manage a problem inherent in narrow FOV star trackers: the huge variation in the nature of the starfields encountered. A given field may be sparse (having few or no stars above the faint limit), crowded, dominated by large objects (globular clusters or a nearby galaxy), dominated by a very bright star or planet, etc. By having the more complex attitude determination tasks directly accessible through the scripting language, ground controllers can tailor the observing scripts to handle the idiosyncrasies of each star field rather than having to make the flight software capable of dealing with every possibility. Further information on the IDS attitude determination software and the overall performance of the FUSE attitude control system is given in Ake et al. (2000).[2]

## 2. PERFORMANCE REQUIREMENTS

In order to attain the required pointing accuracy the FES was made an integral part of the optical system of the FUSE science instrument. The FUSE science instrument consists of four co-aligned telescopes and spectrographs mounted on a common graphite-epoxy optical bench. Two of the four telescopes have primary mirrors coated with aluminum and overcoated with LiF, and two are coated with SiC. The primary mirrors and spectrographs are designed to operate at far-ultraviolet wavelengths, but the two mirrors coated with Al+LiF also have excellent reflectivity at visible wavelengths. Further information on the FUV instrument can be found in Sahnow et al. (2000a, 2000b)[3],[4] Ohl et al. (2000),[5] and Brownsberger et al. (2000).[6]

The FES directly views the focal plane of one of the FUSE primary mirrors. The prime FES unit (FESA) is mounted just below the focal plane assembly (FPA) in the LiF1 optical channel, so that the mirrored surface of the FPA slit-plate redirects the light into the FES where it is reimaged onto a CCD detector. A schematic view of the light path is shown in Figure 1 for the LiF1 and SiC1 channels. The redundant FES (FESB) is similarly mounted in the LiF2 channel. A complete visible-light subsystem consists of an FES, an FPA, a primary mirror, and the baffle tube assembly that protects the optics from stray light. This arrangement provides several natural advantages: rigid coalignment of the FES with the instrument optical axis, direct measurement of the optical axis by measuring the slit positions in the FES field of view, and a large light-collecting area. The large collecting area is particularly important: the need to measure star positions with sub-arcsecond precision effectively limits the size of the FOV ($\sim 19'$ square for the FUSE FES), hence only faint stars will be visible for most lines of sight. In particular, the FUSE FES must be able to meet its requirements for stars as faint as V=13.5 mag.

The main operational requirements for the FES can be summarized briefly as follows. The FES shall:

- provide full FOV images that are between $17'$ and $21'$ square, binned by a selected factor (1, 2, 4, 8)
- have the FOV offset by 5.5 arcminutes from the optical axis (to accomodate limitations on baffle placement)
- have a PSF RMS radius $< 5$ arcseconds in each axis
- accomodate changes in focus of the primary mirror of up to 100 microns (the approximate net effect from 1-G release and shrinkage of the telescope structure from water desorption on orbit)
- provide centroids of up to 6 selected point sources, each with a noise equivalent angle (NEA) $\leq 0.2$ arcseconds for stars brighter than V=13.5 and with color B-V $> 0.5$.
- provide centroids at adjustable intervals; the NEA requirement must be met at fixed intervals of 1 or 2 seconds
- deliver centroid data $< 0.7$ seconds after completion of the exposure
- have the exposure duration selectable over the range 0.05 to 60 seconds
- be able to image point sources with $0 < V < 16$ without saturation
- be able to provide unsaturated images of the planets other than Mercury
- be able to image comets with surface brightness $> 15$ mag per square arcsecond
- accept commands and provide telemetry in the form of CCSDS packets, using a MIL-STD 1553 bus interface

The implementation of these requirements is described in the subsequent sections.

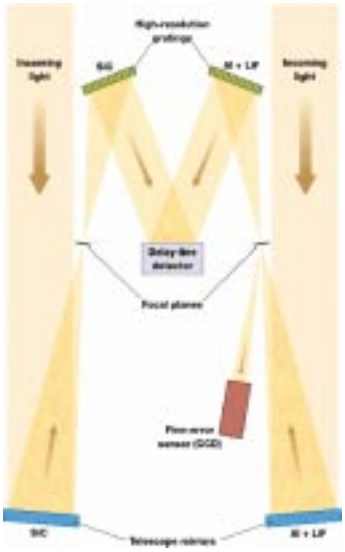

**Figure 1.** A schematic illustration of the light paths for the LiF1 and SiC1 channels of the FUSE instrument is shown. This figure is not drawn to scale; in particular, the FES is mounted much closer to the FPA than shown here.

## 3. IMPLEMENTATION

Each FES is composed of three subassemblies: the camera assembly, containing the optics, CCD detector, and preamps; the controller assembly, containing all the remaining electronics and external electrical interfaces, and a radiator and heat strap used to cool the CCD. The three subassemblies are shown in Figure 2.

### 3.1. Optics

#### 3.1.1. Design

The FES optical system is optimized for accuracy in centroiding. The NEA requirement can be met with a practical number of detector pixels only by having the PSF larger than 1 pixel and centroiding the resulting signal to sub-pixel precision. This means the optical design must include aberrations in a controlled manner so that the PSF is large (FWHM $\approx$ 1.5-2 pixels) and uniform across the field of view. The PSF must also not be too large, because then the signal from faint stars will be too easily lost in the presence of background.

No internal focus adjustment mechanisms were included in the FES, in part because of cost and schedule constraints, in part because of the limited volume available for the camera assembly, and in part because only a limited range of focus adjustment (100 microns) was expected to be required. Instead, the choice was made that the optical design had to produce a PSF that was insensitive to the expected changes in focus, and that the FES would have to be carefully aligned and focussed at the time it was installed on the telescope.

The input beam to the FES is produced by one of the FUSE off-axis paraboloid primary mirrors and a flat folding mirror (the FPA slit-plate). The FES optics consist of a parabolic primary mirror, a hyperbolic secondary mirror, a filter wheel, an achromatic field-flattening doublet, and a windowed CCD detector. This system corrects for the coma introduced by the FUSE primary mirror and produces images with the desired PSF. The distortion in the field is small (exceeding 1% only in the corners of the FOV farthest from the optical axis), and is accurately corrected by means of a polynomial in the IDS software. A field stop is located at the surface of the FPA mirror to prevent any light that might be scattered by baffle vanes from entering the FES. This field stop reduces the FOV slightly, from $21'$ square to about $19'$ square. The interior of the FES camera assembly is shown in Figure 3.

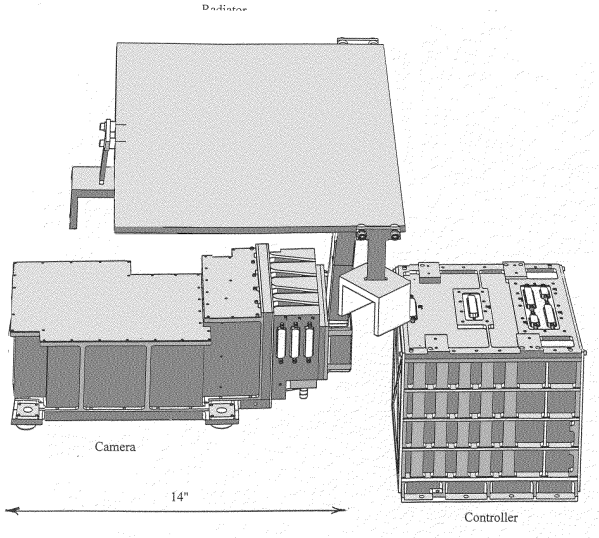


**Figure 2.** This figure shows the relative placement of the FES assemblies for FESA. The LiF 1 FPA would be to the left and behind the upper left corner of the camera in this view. The U-shaped channels on which the radiator flexures are mounted are bonded to cross-braces in the FUSE instrument structure.

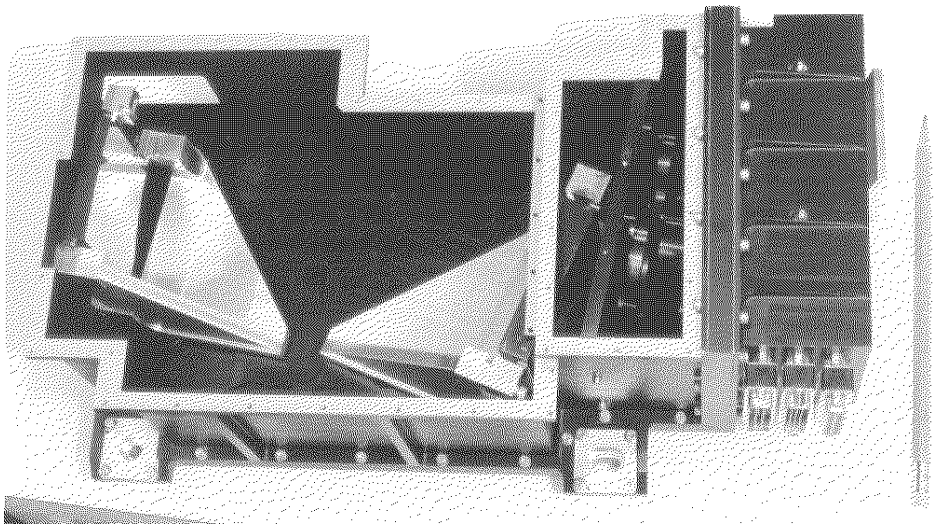

**Figure 3.** The interior of the FES engineering qualification model is shown. The entrance aperture is to the upper left. The main components, from left to right, are the secondary mirror, the primary mirror, a light baffle, and the filter wheel mechanism. The doublet is mounted within the wall to the right of the filter wheel. The CCD cavity enclosure is in place so the CCD itself is not visible. Photo courtesy of CSA.

### 3.1.2. Image Quality

Verification of the proper alignment of each FES following installation was straightforward, but verification of the focus was problematic. FES images of the slit-plates indicated that the focus was correct to within a few hundred microns. This was adequate to ensure that the focus was well within the range of motion of the FPA's and primary mirrors but not adequate to ensure that the FUV and visible light optical systems could be optimized simultaneously. A proper focus test would have required full-aperture illumination of the FUSE primary mirrors by light that was collimated to $1''$ or better. Such a test was deemed impractical during FUSE integration because of the difficulty of the test setup and because the need to minimize exposure of the LiF-coated optics to ambient air made it difficult to provide full-aperture illumination of the FUSE primary mirror. The optical testing issues are discussed in greater detail by Conard et al. (2000).[7]

Initial on-orbit images from FESA showed it to be in almost perfect focus, with PSF widths of 1.5 to 2.0 pixels FWHM (there is a slight but noticeable variation in PSF width with position in the FOV). However, the LiF1 mirror was subsequently moved by 200 microns in order to improve the spectral resolution of the FUV data, causing the PSF width to increase to 2.5 - 3.5 pixels FWHM. FESA was operated in this state for 5 weeks, but we found that the larger PSF resulted in occasional field identification and tracking problems for guide stars near the faint limit. Consequently, we adjusted the FPA focus position by 100 microns to restore the FESA PSF to its original size. This results in some loss of throughput for FUV data obtained in the LiF1 channel using the narrow slit, but this slit is seldom-used and overall observing efficiency is greater by having the FES working optimally.

For FESB, initial on-orbit images showed a doughnut-shaped PSF with a diameter of 5-6 pixels. Comparison with ray-traces indicates that FESB could be brought into ideal focus by moving the LiF2 primary mirror 600 microns, moving the LiF2 FPA by 300 microns, or some combination of the two. Thus, if FESA were to fail the LiF2 channel optics could be adjusted so that FESB provided equally good guiding with only a modest degradation of the FUV capabilities of that channel. These tradeoffs were considered explicitly in the choice not to include an internal focus mechanism in the FES. All other characteristics of FESB are essentially identical to those of FESA.

Two images from FESA with fairly crowded star fields are shown in Figure 4. The image of the $\eta$ Carina region also includes the prominent reflection nebula NGC 3372, which is clearly seen even in a 1-second exposure. The vertical streaks in the $\eta$ Carina image are caused by light from the brighter stars in the image falling on each pixel in a column as the image is transferred to the storage region of the CCD prior to readout. The effective exposure time for each pixel during frame transfer is $1/5000^{th}$ of a second. The brightest streak, from the $7^{th}$ magnitude star BO Carina, has an intensity of about 100 ADU/pixel. Such streaks have no effect on the IDS image processing software. The dense OB association NGC 346 contains several stars that are part of the FUSE observing program. Despite the crowded nature of the field, these stars were successfully acquired and observed using routine procedures.

### 3.1.3. Filters

There is a three-position filter wheel located between the FES secondary mirror and the doublet lens. The three filters available are: a clear filter, a neutral density filter for use with very bright objects, and a broad-band color filter. The clear filter has been used for all guiding thus far into the mission. The neutral density filter transmission is 0.2% at 400nm and rises almost linearly to 0.8% at 900 nm, providing a typical mean attenuation of almost 6 magnitudes. The broad-band color filter is different in each FES. The filter in FESA corresponds roughly to a standard V band: its transmission is approximately 93% between 470 nm and 620 nm and drops abruptly outside this range. The FESB color filter corresponds roughly to an R-band filter: its transmission is approximately 90% from 600nm to 800nm and drops quickly to zero outside this range.

### 3.1.4. Internal scattering

The observation of very bright objects, such as stars up to V=0 and planets (V ranging from -2 to -4), poses a severe challenge. An unsaturated image of such bright objects can be obtained by use of the neutral density filter and by reducing the exposure duration, but then none of the other stars present in the FOV will be visible for guiding. If the clear filter is used and the exposure time set to normal values, then the scattering of light from the bright object by the various optical surfaces can increase the background to the point that the relatively faint guide stars are unusable. In addition, the spatially varying background produced by such scattering has the potential to confuse the star detection software. Measurements performed pre-flight demonstrated that the system met its requirements, but there were no means to determine the contribution of the test equipment to the observed scattering profile.

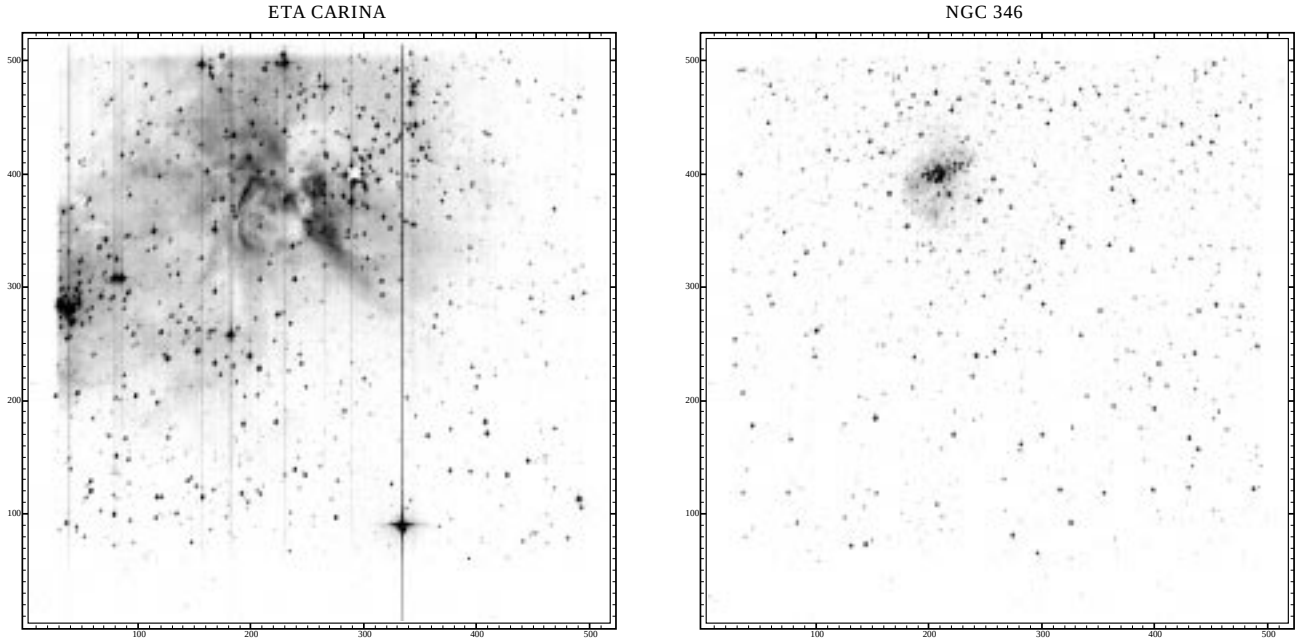


**Figure 4.** Two sample FES images are shown. The left panel shows the field surrounding the star $\eta$ Carina, the right panel the field surrounding the OB association NGC 346 in the Small Magellanic Cloud. The reflection nebula NGC 3372 shows up clearly in the left panel despite the short 1-second integration time. The vertical streak in the left panel is caused by light from the 7th magnitude star BO Carina falling on the pixels in that column as the image is transfered into the storage region of the CCD. The bright star $\eta$ Carina is not seen, as its light is passing through the $30''$ aperture in the FPA slit-plate. This aperture is located at X=290, Y=400, and can be seen as a white square against the nebulosity. Faint diffraction spikes from the star are visible. The faint nebulosity surrounding the NGC 346 OB association can also be seen. Stars as faint as $17^{th}$ magnitude can be detected in each image.

In-flight measurements of bright stars have shown that the visible light scattering properties of the FUSE optics are excellent. For example, an image of the V=0 star Vega obtained using our standard procedures (clear filter, 1-second exposure time) showed a radial scattering profile that had fallen to 400 ADU/pixel at a distance of 2 arcminutes and 100 ADU/pixel at a distance of 4 arcminutes. The signal from the star itself is $\sim 4.7 \cdot 10^8$ ADU/sec under these conditions. We can therefore track guide stars even at the faint limit as long as they are at least a few arcminutes distant from a bright source. The star detection and identification software is not 100% reliable in such cases however, so target acquisitions are presently done on offset fields for sources brighter than V=1.5, followed by a small slew to the target field and direct acquisition of pre-selected guide stars.

### 3.1.5. Stray Light

The primary source of background in the FES is stray light from the day side of the earth. This background varies slowly with orbit phase, with a maximum at orbit "noon", and varies strongly with the angle of the telescope line of sight relative to the horizon (the "earth limb" angle). The nominal requirement is that the telescope baffles reduce the stray light to the point that the NEA requirement can be met for guide stars at the faint limit for bright earth limb angles as low as 15 degrees. In practice, limits on placement of the FUV optics and the size of the launch vehicle fairing precluded use of deep vanes in the baffles and prevented the baffle tubes from extending the full height of the instrument. As a result, the stray light exceeds the requirements for limb angles below about 25 degrees, and can be as high as 10000 ADU/pixel/sec for a limb angle of 15 degrees at orbital noon. The stray light intensity is plotted as a function of orbit phase and earth limb angle in Figure 5. The main impact on operations has been to constrain the times at which target acquisitions occur; there have been only a few cases throughout the mission where we have lost

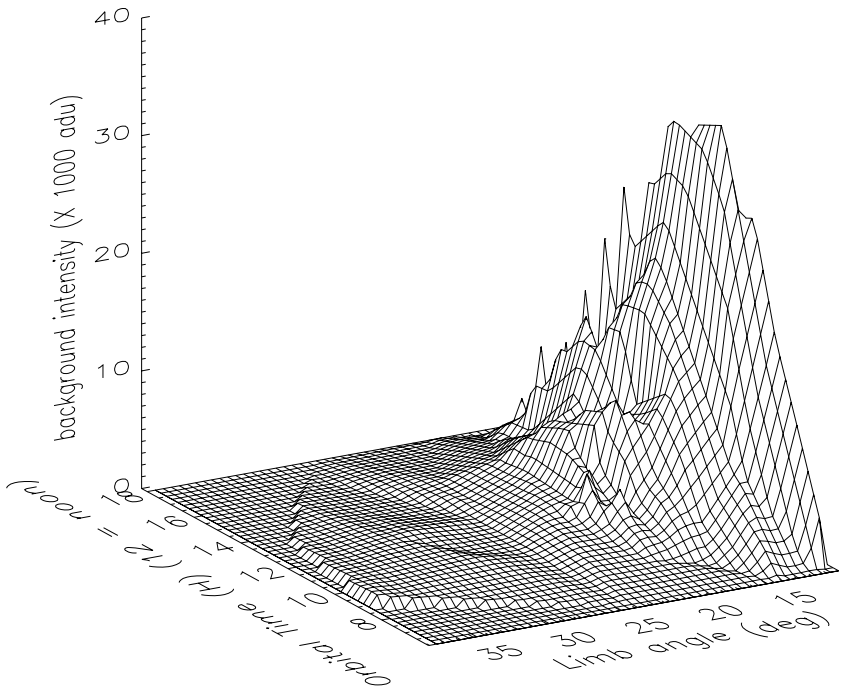


**Figure 5.** The stray light background in the FES is plotted as a function of bright-earth limb angle and orbital phase. The satellite crosses the terminator from night into day at a phase of about 6 hours on this plot, and crosses back into night at about 18 hours. The background is negligible on the night side of the orbit.

lock on guide stars due to stray light after they were successfully acquired. The satellite orientation is maintained so that the LiF baffles are shaded from the sun, so stray sunlight is not a source of background in the FES.

### 3.2. CCD Detector

The CCD detector is a modified version of a SITe SIA003A. This is a 1024x1024 pixel thinned backside-illuminated CCD die mounted on a 2-stage thermo-electric cooler (TEC) and sealed in a kovar package with a fused silica window. The main modification to the standard device was to apply an opaque mask that covered half the rows on the CCD, so that by operating half of the split serial register the result is a 512x512 pixel frame-transfer device. Each FES uses a different half of the physically-available 512x1024 pixel imaging area.

Many basic characteristics of the CCD are given in Table 1. The clock rates are governed by the FES software and could be changed if the need arose. The QE shown was measured at -55C; higher values are obtained at room temperature. The end-to-end system sensitivity is given in Table 2. The CCD is ordinarily operated in MPP mode, but non-MPP mode may be selected if desired. The mean dark current has increased significantly in the course of 1 year of operations, from 4 to 33 $e^-$/pixel/sec. Radiation damage has also created a number of "warm" pixels. About 4500 pixels ($\sim$1.7%) have dark current elevated by <30 ADU/pixel/sec, about 70 pixels have dark current elevated by 30 - 150 ADU/pixel/sec, and about 20 pixels have dark current elevated by 150-600 ADU/pixel/sec. This increase in dark current has not yet had an adverse impact on performance. Preliminary tests have been performed in which the decontamination heater (see Section 3.5 below) is used to anneal the hot pixels by raising the die temperature to +30C. These tests have found that as little as 3 hours of annealing greatly reduces the dark current in the warm pixels. Further tests are continuing to determine the most efficient annealing procedure. Hot pixels also can be corrected in software if necessary (see Section 3.6 below).

### 3.3. Electronics

All FES electronics, with the exception of the CCD and its preamps, are located in the controller asembly. The main functional elements are the CPU, memory, CCD clock-generation, analog signal processing, the MIL-STD-

**Table 1.**

| CCD Characteristics | |
|---|---|
| Pixel Size | 24$\mu$m |
| Read Noise | 7 $e^-$ |
| QE @ 700nm | 55% @ 400nm, 65% @ 700nm, 37% @ 900nm |
| Gain | 5 $e^-$ / ADU |
| Full Well | 280,000 $e^-$ |
| Digitization rate | 50 Kpixels/sec |
| Parallel Clock rate | 5000 lines/sec |
| Dark current (MPP) | 4.1 $e^-$/pixel/sec at -30C (preflight) |
| Dark current (MPP) | 33 $e^-$/pixel/sec at -32C (1 yr post-launch) |

1553 bus interface, and secondary power supplies. There are also control circuits for the filter wheel, TEC, and decontamination heater.

The processor is a radiation-hardened 68020 CPU operating at a clock speed of 17 MHz, along with a 68882 floating point unit. The memory available consists of 1 Mbyte of RAM for program execution and working memory, 2 512 Kbyte banks of EEPROM for program storage, 128 Kbytes of PROM for the boot code, and 128 Kbytes of EEPROM for storage of CCD control waveforms. A complete copy of the operating system and application code is stored in each bank of EEPROM. Thus a new version of the code can be uplinked and stored in one bank of EEPROM without disturbing the version stored in the other bank. One such upload has been performed since launch. The processor and memory described above (except for the CCD waveform EEPROM) is physically identical to that in the IDS, resulting in reduced overall cost and development schedule. Each FES has experienced one watchdog reset since launch, apparently caused by a single event upset (SEU) in the processor. This is consistent with prelaunch estimates based on the radiation environment and characteristics of the parts chosen.

The state of the CCD clock levels at any particular moment in time is determined by a control register. The execution of a CCD readout has been decomposed into a small number of standard clocking patterns such as a single parallel shift of image and storage registers, or a shift of just the storage register, or a serial transfer with/without data sample, etc. Each of these patterns, or "macros", is stored in the CCD control waveform EEPROM.

Before any particular readout mode can begin, the CPU determines the order in which macros need to be executed for that particular mode, and saves the results in a table in memory. During execution, the table is passed serially to FPGAs on the CCD clock generation board, which mediate the transfer of the clocking words from memory to the CCD clocking hardware, as well as the timing of ADCs and various elements of the analog signal processor hardware.

Through the use of primitive macros, the CPU can easily create flexible readout patterns capable of reading out the full imaging area of the CCD or of quickly skipping rows and pixels to read out only the desired regions of interest. This scheme achieves good performance with a minimum of memory. It also has the flexibility to fine-tune performance throughout the development process, as well as to modify in minute detail the operation in orbit, such as might be required to overcome trapping time constants in the CCD as a result of in-flight radiation damage.

The ability to read out only small regions of interest is essential in order to meet the FUSE pointing performance requirements. The ACS requires attitude updates at 1 Hz that utilize the full noise and sensitivity capabilities of the FES. This cannot be achieved if the entire CCD is digitized for each update, so the software makes use of these macros to digitize only small subimages at the locations of selected guide stars. The resulting clock waveforms are unique to each target observed by FUSE.

The analog signal from the CCD is processed using correlated double sampling. The timing of the clamp signal in the sample and hold amplifier and the ADC conversion cycle are controlled by the same macros used to generate the CCD clock signals. The ADC used (CS5101A) digitizes the signal to 16 bits with very low non-linearity.

Total power consumption, excluding the TEC and decontamination heater, is 16.9 watts. The TEC typically consumes 0.5 - 1 watt, but may run as high as 5 watts depending on the setpoint. The decontamination heater power consumption is 30 watts. Each CCD also has a thermostatically-controlled 5-watt survival heater, but in flight the CCD has never been cold enough for this heater to be energized.

### 3.4. Thermal and Mechanical Issues

The thermal and mechanical design issues are closely coupled in the FES. In addition to the usual concerns of surviving launch-induced vibration loads and dissipating heat generated in the electronics, the design has to provide for maintaining alignment of the FES optical components (both internally and with respect to the full FUSE optical system), and for cooling of the CCD.

The vast majority of electrical power is consumed in the controller assembly; component temperatures in the controller are managed by standard heatsinking to the chassis. The chassis in turn is mounted on a baseplate that is regulated by a combination of external radiators and heaters. The only power consumption in the camera assembly during normal operations is in the CCD die, a nearby preamp, and the TEC mounted in the CCD package. The are also infrequent brief pulses to the filter wheel mechanism that do not affect the thermal balance of the camera. No heaters are used to regulate the camera temperature: its temperature is defined by conduction of the mounting pads to the spectrograph structure and radiation to nearby components (spectrograph structure, FUV detector, etc), all of which are regulated to $\pm 1^{\circ}$C.

The FES mirrors, their brackets, and the camera housing are all aluminum so as to provide a nearly athermal design. The mirrors are fabricated with integral flexure mounts, which are pinned to a bracket that is in turn pinned to the camera baseplate. Positioning of the mirrors and the doublet lens is done solely by means of tight machining tolerances; the only adjustable element is the CCD package. The CCD and a small preamp board are mounted to the camera frame by means of 3 spring-loaded adjusting screws and a set of locking screws. The CCD was aligned and focussed prior to FES environmental testing and was not adjusted thereafter. Differential thermal expansion of the camera baseplate and spectrograph structure was handled by means of a three-hole mounting scheme that approximated a kinematic mount: one baseplate mounting pad contained a close-tolerance hole, one a close-tolerance slot, and one an oversize hole. This permits the camera housing to expand and contract without introducing any distortions.

Cooling of the CCD is done primarily by an external radiator, with some assistance from a TEC. The CCD package is coupled to the external radiator by means of a heat strap fabricated from flexible copper braid that was fused at either end into a copper block. The large mass of the copper heat strap posed some design challenges in that it had to have good thermal contact with the CCD package while not introducing any mechanical loads that might disturb the CCD alignment. Substantial brackets were thus required to support the heat strap during launch, but these brackets had to be designed so that they would not introduce thermally conductive paths between the cold heat strap and the warm structure after launch. Thermal isolation of the heat strap and CCD assembly from the warm structure and camera housing was achieved by using titanium for all brackets and screws, and G-10 or ultem for insulating spacers. The strap was wrapped in a 15-layer thermal blanket to minimize radiative coupling. The connection between the CCD package and heat strap was obtained with a small copper block that was machined so as to form leaf springs in both transverse directions; this provided high thermal conductivity while minimizing mechanical coupling. Chotherm gaskets are used to improve the thermal conductivity at each interface in the thermal path between the radiator and the CCD. The CCD itself and the interior walls of the CCD cavity in the camera had low emissivity surfaces to minimize radiative coupling to the CCD.

The external radiator has a surface area of approximately $0.14\,\mathrm{m}^2$, and its front surface is coated with silver teflon to provide high emissivity and low absorptivity. It is mounted to the structure via 3 titanium flexures and G-10 insulating spacers. The rear surface of the radiator is isolated from the instrument by a thermal blanket. The spacecraft attitude is always maintained so that the radiator of the active FES is shaded from the sun.

The actual temperature that can be achieved at the CCD die varies with spacecraft attitude; we have chosen to operate at a conservative temperature of -32C, which can be achieved at all attitudes. This is limited largely by parasitic heat loads from the instrument structure: during in-orbit checkout the instrument thermal environment was maintained roughly 10C below the present temperatures, and the CCD die temperature could be reduced to -40C.

It is possible that the parasitic losses could have been significantly reduced if the mass of the heat strap had been lower. This would have permitted smaller mechanical supports for the heat strap, and we might have been able to eliminate one or both of the intermediate support brackets entirely. We investigated the use of graphite fiber materials in place of copper, but concluded that the uncertainties in procurement time and the need for more extensive development and prototyping could not be accomodated in the overall FES delivery schedule.

### 3.5. Contamination

The FUV waveband (900Å - 1180Å) under study by FUSE imposes stringent contamination requirements, especially for molecular outgassing. Very few materials are acceptable in the fabrication of components in the FUSE optical cavities, and rigorous cleaning and handling procedures were followed throughout assembly, integration, and test. A larger but still carefully-controlled list of materials is acceptable for components outside the optical cavities (primarily electronics), but vent paths were carefully chosen to minimize any chance that molecular gasses could migrate to the optical cavities. The interior of the FES camera was effectively a part of the FUSE FUV optical cavity, so it was subject to the same requirements. Meeting these requirements for the camera housing, optical elements, and optical mounts was fairly straightforward. The filter wheel mechanism, however, was an existing design that required some modifications. Some materials were changed (primarily lubricants), and the outer case was sealed apart from a vent tube that extended directly into the instrument electrical cavity.

The cold temperature at which the CCD operates creates some contamination concerns unique to the FES. The CCD and its window are by far the coldest surfaces in FUSE, so any vapors present will preferentially condense onto it. Such condensation could distort the images obtained by the FES and possibly prevent it from functioning, so two different approaches were employed to avoid this problem. First, we tried to minimize the exposure of the CCD to any potential sources of condensable vapor (primarily water). The CCD and its electronics were mounted in a sealed enclosure that was connected to the instrument nitrogen purge lines and had a dedicated vent tube that extended outside the instrument thermal blankets. The CCD cavity was isolated from the rest of the camera by means of a solid wall in which the doublet lens was mounted. The CCD cavity was thoroughly baked-out and was subsequently kept under nitrogen purge until launch. Second, a dedicated 20-watt heater was mounted on the CCD case to be used for evaporating any material that did condense onto the CCD window during flight. This heater was also intended for annealing hot pixels in the CCD caused by radiation damage. The precautions taken to avoid condensation onto the CCD window have proven successful: after one year of flight operations there is no evidence for condensation.

### 3.6. Software

The VRTXsa operating system (Microtec Research) provides the software environment for the FES. The application code is written in C and consists of a series of event-driven task-oriented modules that communicate by means of shared data structures. All commands and telemetry are transmitted as CCSDS packets over the MIL-STD-1553 bus connecting the FES to the IDS. All internal FES timing is synchronized to the arrival of a time code packet sent from the IDS at 1 Hz containing the present UTC.

Upon power-up or issuance of a watchdog reset the FES loads boot code from PROM. The boot code performs a series of self-tests on the hardware, reports the results in a housekeeping telemetry packet, and waits for commands. The only valid commands in boot mode are to upload data to memory or to copy application code from either EEPROM to RAM and begin execution of the application code.

Imaging by the FES is controlled by means of image configuration and exposure control commands. For full field of view images, the configure command specifies the degree of on-chip binning to be performed (images may be binned by 1, 2, 4, or 8 pixels in each dimension). For subimages, the configure command specifies the location and size of each subimage, as well as the type of processing to perform on each subimage. The exposure control command specifies the duration of the exposure, its timing relative to the 1 Hz clock pulse, and the interval between exposures when doing centroiding. The configure commands are used to construct the macro sequences for clocking the CCD, and the exposure control command governs the relative timing of the different macro sequences. When centroiding, the macro sequences will cause only those pixels in the selected subimages to be digitized: rows not containing a subimage are flushed, and pixels in a row that contains a subimage but that are outside the subimage are also flushed. A commandable number of pixels in each row preceding the desired pixels are digitized and discarded so as to avoid transients in the analog signal processing electronics.

Several processing steps may be applied to subimage data prior to computing the centroid: 1) dark current subtraction, 2) bad pixel masking, 3) cosmic-ray removal, and 4) thresholding. Both the dark current subtraction and the bad pixel removal make use of the bad pixel mask that can be uploaded to the FES. If a "hot" pixel is specified in the mask, the value given is scaled by the exposure time and subtracted from the signal in the pixel. If a pixel is flagged as "bad" in the mask, the signal in that pixel is replaced by the mean of the surrounding pixels. At present, no bad pixels have been identified, and none of the "warm" pixels that have appeared as the result of radiation damage is yet strong enough to warrant correction. Cosmic ray removal is performed by comparing the

pixel values in a subimage with those in the preceding subimage. If a pixel signal exceeds that in the previous image by more than a specified multiple of the RMS error in the previous pixel signal, it is replaced by that previous value. This algorithm has worked well, allowing us to track guide stars through every passage of the South Atlantic Anomaly. The thresholding step subtracts the threshold from each pixel and sets resulting negative values to zero. The threshold is computed by calculating the mean signal in the perimeter of the subimage and adding a specified multiple of the RMS signal. This step is crucial for maintaining the required NEA in the presence of the large stray light background encountered on the day side of the orbit. Finally, the centroid of the remaining signal in the subimage is calculated and reported to the IDS.

No processing of full field of view images is performed by the FES: detection of stars, background removal, and centroiding are all performed by the IDS. Full field of view images include 8 rows and 8 columns of overscan, which can be used by ground calibration software for determination of bias levels, readnoise, etc.

The use of operating system calls for various aspects of task execution and interrupt servicing does have a subtle effect on the full FOV images. A 50-pixel FIFO buffer is used in the interface between the ADC and the image data buffer in RAM. The operating system overhead in interrupt servicing results in this FIFO filling completely and CCD readout being halted while the FIFO is emptied. This interruption in CCD readout introduces a small shift in the bias level of the first pixel to be digitized after the FIFO is emptied. This bias level shift is typically a few tens of ADU, and the FES software adds a commandable value to every 50th column in an image to correct for this effect. The magnitude of the offset does vary with the binning factor in effect during readout. The largest subimage available is 25 pixels, so this effect is not present when centroiding.

The interruption in the CCD readout at every $50^{th}$ pixel has a similar effect if there is a source in the FOV that is bright enough for charge to bleed down the columns to the serial register. In this case the charge leaking into the serial register raises the overall bias level in the image and there will be extra signal in every 50th column. This effect appears when there is a source in the FOV brighter than V=1-2 for 1x1 binned images, depending on the location of the source in the image. For 2x2 binned images, with their shorter readout time, the effect appears for sources brighter than about V=0.5. The readout time for subimages is so short that the effects of charge bleeding from a bright source are insignificant.

A large fraction of the instrument data bus schedule is devoted to FES data. The IDS polls the FES 25 times each second for the presence of updated centroid data so as to minimize latency in computing an updated attitude estimate for transmission to the ACS. Roughly 40% of bus schedule, moreover, is devoted to FES image data. An unbinned full FOV image is 0.5 Mbyte in size, and requires 37 seconds to transmit over the bus. During this time the satellite is drifting on gyros, and if the drift exceeds half the size of the subsequently commanded subimages then it will not be possible to lock onto the guide stars found in the image. This has occurred only when many hours have passed without FES centroid data, but in order to make operations as robust as possible we now routinely perform target acquisitions on images that have been binned 2x2 to reduce the bus transit time to under 11 seconds.

## 4. FES PERFORMANCE SUMMARY

The performance characteristics of the FUSE visible light subsystem are summarized in Table 2 below. The sensitivity value shown in the table is an average over approximately 1000 guide stars with V magnitudes as given in the Hubble Guide Star Catalog (GSC). The actual signal obtained from a given star may differ by a factor of 2 from what would be estimated from the mean sensitivity, in part from the uncertainties in the GSC magnitudes and in part from the variation in FES response with stellar color. The centroid rate entries show the typical operating configurations employed. The time required to read out subimages limits the possible combinations of subimage size, number, and exposure time. The 1 Hz mode with 10x10 subimages is the default; 16x16 subimages are used when the target acquisition includes a peakup, as that entails small slews that might move the guide stars out of 10x10 subimages. The 0.5 Hz mode with the longer exposure time is used when all the guide stars are at or near the faint limit.

The key parameter is the NEA, which comfortably exceeds its requirement. The pointing stability of the FUSE satellite has typically been 0.35″ FWHM over the first year of operation. More generally, the FES has met or exceeded all of the requirements tested after one year of flight operations. Two requirements have not yet been tested: the ability to provide unsaturated images of planets and to image comets brighter than 15 magnitudes per square arcsecond. Based on the FES performance with point sources, we expect these last two requirements will also be met when observations of such objects are scheduled later in the mission.

**Table 2.**

| FES Characteristics | |
|---|---|
| FOV | $19.3' \times 18.3'$ |
| Plate scale | $2.55''$/ pixel |
| NEA (typical) | $\leq 0.15''$ |
| Sensitivity (typical) | 9350 $e^-$/sec @ V=13.5 |
| PSF | $5''$ FWHM |
| Exposure time | 0.048 - 300 sec |
| Subimage size | 3 - 25 pixels square |
| Centroid rate | 6 10x10 subimages @ 1 Hz $T_{exp} = 0.4\,s$ |
| | 4 16x16 subimages @ 1 Hz $T_{exp} = 0.4\,s$ |
| | 6 16x16 subimages @ 0.5 Hz $T_{exp} = 1.2\,s$ |

## ACKNOWLEDGMENTS

We would like to thank the staff at COM DEV for their careful work in performing the detailed design, fabrication, and qualification of the Fine Error Sensors. The Fine Error Sensors were contributed to the FUSE project by the Canadian Space Agency. FUSE is a joint NASA-CNES-CSA mission operated by the Johns Hopkins University. Financial support to U.S. participants has been provided by NASA contract NAS5-32985.

## REFERENCES

1. B. K. Heggestad and R. C. Moore, "The far ultraviolet spectroscopic explorer instrument data system," *Proc. 18th Digital Avionics Systems Conference* , 1999.
2. T. B. Ake, H. L. Fisher, J. W. Kruk, P. K. Murphy, and W. R. Oegerle, "Fuse attitude control: Target recognition and fine guidance performance," *Proc. SPIE* **4139**, p. these proceedings, 2000.
3. D. J. Sahnow, H. W. Moos, T. B. Ake, B.-G. Andersson, M. Andre, D. Artis, A. F. Berman, W. P. Blair, K. R. Brownsberger, H. M. Calvani, P. Chayer, S. J. Conard, P. D. Feldman, S. D. Friedman, A. W. Fullerton, G. A. Gaines, J. C. Green, M. A. Gummin, J. B. Joyce, M. E. Kaiser, J. W. Kruk, D. J. Lindler, D. Massa, E. M. Murphy, W. R. Oegerle, R. G. Ohl, S. N. Osterman, B. A. Roberts, K. C. Roth, R. Sankrit, K. R. Sembach, R. L. Shelton, O. H. W. Siegman, H. A. Weaver, and E. Wilkinson, "On-orbit performance of the far ultraviolet spectroscopic explorer (fuse)," *Proc. SPIE* **4013**, p. in press, 2000.
4. D. J. Sahnow, H. W. Moos, S. D. Friedman, W. P. Blair, S. J. Conard, J. W. Kruk, E. M. Murphy, W. R. Oegerle, and T. B. Ake, "Far ultraviolet spectroscopic explorer: 1 year in orbit," *Proc. SPIE* **4139**, p. these proceedings, 2000.
5. R. G. Ohl, R. H. Barkhouser, S. J. Conard, S. D. Friedman, J. Hampton, H. W. Moos, P. Nikulla, C. M. Oliveira, and T. T. Saha, "Performance of the far ultraviolet spectroscopic explorer mirror assemblies," *Proc. SPIE* **4139**, p. these proceedings, 2000.
6. K. R. Brownsberger, J. P. Andrews, G. Allison, and J. C. Westphall, "Performance of the far ultraviolet spectroscopic explorer focal plane assemblies," *Proc. SPIE* **4139**, p. these proceedings, 2000.
7. S. J. Conard, R. H. Barkhouser, S. D. Friedman, J. W. Kruk, H. W. Moos, R. G. Ohl, and D. J. Sahnow, "Far ultraviolet spectroscopic explorer optical system: Lessons learned," *Proc. SPIE* **4139**, p. these proceedings, 2000.